Research Article

Journal of Environmental Nanotechnology

Corrosion Inhibition of Copper in Acid Media using Sparfloxacin – an Electrochemical Study

P. Thanapackiam*, E. P. Subramaniam
Department of Chemistry, Coimbatore Institute of Technology, Coimbatore, TN, India
Received: 18.10.2018 Accepted: 02.12.2018 Published: 30-03-2019
*pthanapackiam@rediffmail.com

ABSTRACT

The inhibitory efficacy of sparfloxacin on copper corrosion in acid solutions has been investigated using the potentio-dynamic polarisation method and electrochemical impedance spectroscopy. Sparfloxacin had a high inhibition effectiveness, and the inhibitory activity was mixed in nature but mainly cathodic in character. The mechanism of the inhibitor's adsorption onto the metal surface has been investigated using potential zero charge investigations. The activation energy (E_a) and thermodynamic parameters such as the adsorption equilibrium constant (K_{ads}), the free energy of adsorption (ΔG_{ads}), S and H were estimated using the temperature-dependence of corrosion rates. The free energy of adsorption close to -40 $kJmol^{-1}$ has indicated that the adsorption was through electrostatic coulombic attraction and chemisorption. Sparfloxacin molecules adhered to the Langmuir adsorption isotherm. The synergistic impact of KCl, KBr and KI has been studied and the inclusion of KI resulted in an increase in inhibitory efficiency owing to synergism.

Keywords: Acid solutions; Copper; EIS; Potentio-dynamic polarization; Sparfloxacin.

1. INTRODUCTION

Copper is an important engineering material and finds applications in electricity, electronics, chemical industry, building construction, ornamental parts, etc. Even though copper is relatively a noble metal, it is susceptible to corrosion in acids. Copper is exposed to the corrosive solution often during processing. The most practical method for the protection against corrosion in acid media is the use of organic inhibitors containing heteroatoms such as N, O, P and S and/or multiple bonds and aromatic rings. Owing to strict environmental regulations, low inhibitor toxicity is an important requirement for the applied inhibitors. Due to sparfloxacin's low toxicity and high efficiency, an attempt has been made in this study to investigate the corrosion inhibition mechanism and efficiency of sparfloxacin for copper corrosion in 1.0 M HNO_3 and 0.5 M H_2SO_4 acid solutions at various concentrations and temperatures, utilising techniques such as polarisation, electrochemical impedance spectroscopy, adsorption studies and surface morphological analyses. The thermodynamic and activation parameters for the adsorption process have been calculated and discussed.

2. EXPERIMENTS

2.1 Materials

Copper specimens having a composition of 99.5 wt. % Cu, 0.116 wt. % Si, 0.019 wt. % Al, 0.003 wt. % Ni and 0.002 wt.% Mn and dimensions - 2.5 cm x 1 cm x 0.1 cm were used for weight-loss measurements.

These specimens were polished successively with emery papers of 1/0, 2/0, 3/0, 4/0 and 5/0 grades, de-greased with acetone and dried. For electrochemical investigations, a Teflon-coated cylindrical copper electrode with an exposed area of 0.2826 cm^2 and the previously stated composition was employed. The surface was polished to a mirror-shine with emery sheets of various grades, then de-greased with acetone and blown dry with nitrogen before these measurements. All experiments were carried out at a room temperature of 301 ± 1 K. All of the compounds were of analytical reagent grade (Sigma Aldrich), E Merck (India), and were not purified further. Stock inhibitor solutions were made in 2.5 M acid solutions, and double-distilled water was utilized throughout.

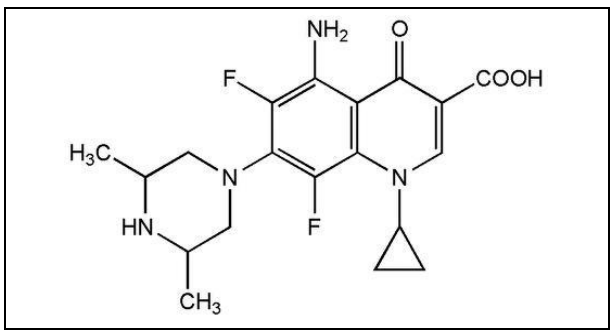

Fig. 1: Structure of Sparfloxacin

2.2 Weight Loss Measurements

According to the American Society for Testing and Materials (ASTM) standard procedure, the weight loss measurements were carried out. The copper specimens, in triplicate, were immersed for a period of 2 h at room temperature (301 ± 1 K) in 100 ml of the corrosive media, both with and without the inhibitor. The average weight loss was used to calculate the inhibition efficiency using the formula:

$$IE = \left(\frac{W-W'}{W}\right) X\ 100 \qquad (1)$$

where, W and W' represent the corrosion rates in the blank and inhibited solutions, respectively.

2.3 Electrochemical Impedance Measurements

For electrochemical investigations, a saturated calomel electrode (SCE) was utilized as the reference electrode, a Pt foil as the auxiliary electrode and a Teflon-coated copper rod as the working electrode, using a three-electrode configuration. After immersing the specimen in the corrosive media for 45 minutes, a stabilization time of 45 minutes was permitted, which was sufficient for E_{ocp}/Vs (SCE) to reach a stable value. Electrochemical impedance measurements were carried out at the open circuit potential (E_{ocp}/Vs (SCE)), using a potentiostat (GAMRY REFERENCE 600), and the data were analyzed using Gamry Echem Analyst Software. The AC frequency was scanned from 100 kHz to 10 MHz, with the excitation signal being a 10 mV peak-to-peak sine wave. The equation was used to compute inhibition efficiencies (IE %) (Doner *et al.* 2011):

$$IE\% = \frac{R_{ct}^{'}-R_{ct}}{R_{ct}^{'}} X100 \qquad (2)$$

where, R_{ct} and $R_{ct}^{'}$ are the charge transfer resistance values in the blank and inhibited solutions, respectively.

2.4 Polarization Measurements

Potentio-dynamic polarisation curves were acquired using the same cell setup at a potential sweep rate of 1.6 mVs^{-1}. The potentials were scanned largely from negative to positive potentials using OCP. Using the connection, the inhibition efficiencies were computed (Shahin *et al.* 2002):

$$IE\ \% = \frac{i_{corr}-i_{corr}^{'}}{i_{corr}} X\ 100 \qquad (3)$$

where, i_{corr} and $i_{corr}^{'}$ are the corrosion current densities in the absence and in the presence of inhibitor, respectively.

2.5 Determination of Activation Energy

In order to measure the activation energy and understand the process of inhibitor adsorption onto the copper surface, potentio-dynamic polarisation tests were carried out in the temperature range 308 K to 328 K in the presence and absence of the inhibitor in both the acid solutions. The Arrhenius equation was used to calculate the temperature-dependence of corrosion rate:

$$i_{corr} = A\ e^{-Ea/RT} \qquad (4)$$

where, i_{corr} is corrosion current density, R is the universal gas constant, A is the Arrhenius pre-exponential constant, T is the absolute temperature, and E_a is the energy of activation.

2.6 Measurement of the Potential of Zero Charge

At 20 kHz AC frequency, electrochemical impedance values were recorded at various applied DC potentials. Double-layer capacitance values obtained were plotted against applied DC potentials and the PZC was obtained from the lowest point of the plot.

2.7 Study of Synergistic Effect

The synergistic effect of halide ions with the inhibitor on corrosion inhibition was studied. Based on Aramki and Hackermann (1969) equation, the synergism parameter was calculated as follows.

$$S_\theta = \frac{1-\theta_{1+2}}{1-\theta_{1+2}^{'}} \qquad (5)$$

where, $\theta_{1+2} = (\theta_1 + \theta_2) - (\theta_1\theta_2)$; θ_1= surface coverage by anion; θ_2 = surface coverage by cation and θ'_{1+2} = measured surface coverage by both anion and cation.

Table 1. Inhibitor efficiency from weight loss measurement for copper in 1.0 M HNO_3 and 0.5 M H_2SO_4 solutions at different concentrations of the inhibitor

Medium	Inhibitor concentration (mM)	Corrosion rate (mmpy)	Inhibitor efficiency (IE%)
1.0 M HNO_3	Blank	47.2162	-
	0.0004	29.4522	37.6
	0.001	21.6986	54.0
	0.002	16.4909	65.0
	0.01	13.3084	71.8
	0.02	10.4732	77.8
0.5 M H_2SO_4	Blank	22.3929	-
	0.0004	10.5889	52.7
	0.001	7.8693	64.8
	0.002	4.9184	78.0
	0.01	2.0252	90.9
	0.02	1.1572	94.8

2.8 Surface Morphology studies

A digital Scanning Electron Microscope was used to examine the surface morphologies of the corroded samples in the blank and in the presence of the inhibitor. All specimen micrographs were obtained at a magnification of 200X. Before recording the SEM picture, these samples were subjected to the same pre-treatment as in electrochemical tests.

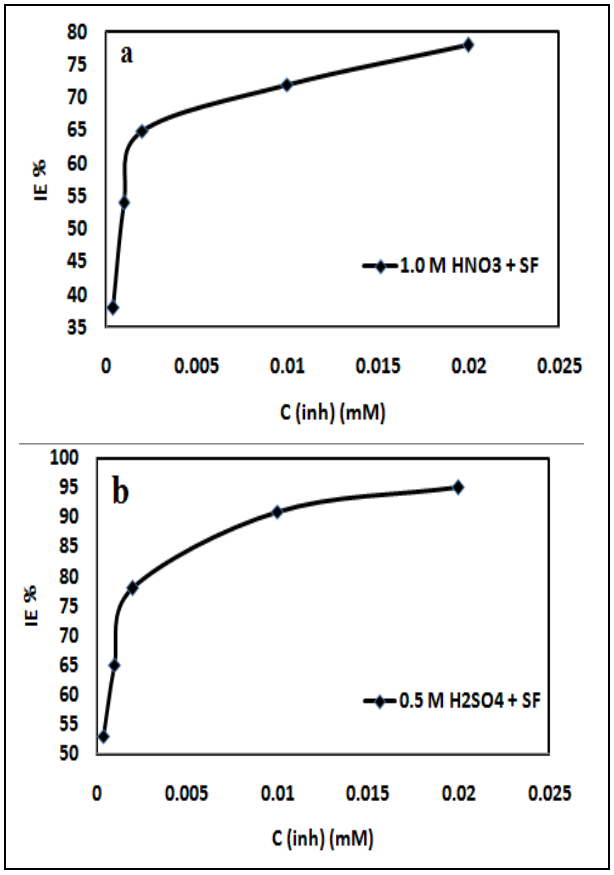

Fig. 2: Plots of inhibitor efficiency (%) with concentration of sparfloxacin in: (a) HNO_3 (b) H_2SO_4

3. RESULTS AND DISCUSSION

3.1 Weight Loss Measurement

Table 1 shows the inhibition efficiency for copper in nitric acid and sulphuric acid medium at various inhibitor doses. As the concentration of the inhibitor increased, there was a sharp increase in inhibitor efficiency at initial doses but however it was tending to attain a steady value with further increase (Fig. 2 a and Fig. 2 b); this was due to the fact that the inhibitor has already covered a significant portion of the surface through adsorption. With the rise in concentration, the curve was tending to flatten out, which was typical of a Type I adsorption isotherm.

3.2 Electrochemical Impedance Study

In 1.0 M nitric acid and 0.5 M sulphuric acid solutions, the impedance spectra obtained at room temperature in the absence and presence of different doses of the inhibitor are shown in Fig. 3 (a and b), respectively.

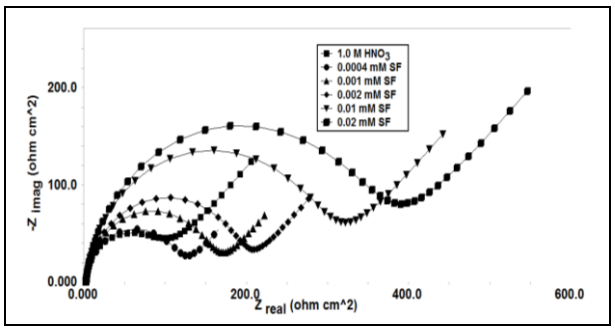

Fig. 3 a: Nyquist plots for Cu electrode obtained in 1.0 M HNO_3 solution at various concentrations of sparfloxacin

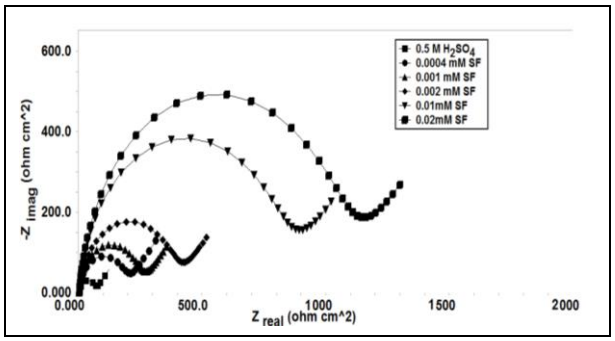

Fig. 3 b: Nyquist plots for Cu electrode obtained in 0.5 M H_2SO_4 solution at various concentrations of sparfloxacin

Table 2. Electrochemical parameters derived from EIS measurements for the corrosion of copper in 1.0 M HNO_3 and 0.5 M H_2SO_4 solutions at different concentrations of the inhibitor

Medium	Inhibitor Concentration (mM)	R_{ct} Ωcm^2	Y0 (x 10^{-6}) $\Omega^{-1}cm^{-2}$	n	C_{dl} μFcm^{-2}	Inhibitor Efficiency (IE%)
HNO_3	Blank	87.0	862.0	0.99	146	-
	0.0004	112.2	682.8	0.95	122	22
	0.001	155.0	401.5	0.93	118	43
	0.002	191.0	192.7	0.92	94.1	54
	0.01	293.2	190.6	0.92	78.5	70
	0.02	356.2	180.5	0.94	63.7	75
H_2SO_4	Blank	63.0	330.0	0.93	159	-
	0.0004	183.0	261.3	0.95	128	52
	0.001	244.2	236.3	0.95	111	64
	0.002	387.0	183.7	0.94	98.2	77
	0.01	820.0	152.6	0.93	81.5	89
	0.02	1061	143.9	0.93	70.9	91

Roughness, chemical inhomogeneities, degree of polycrystallinity and anion adsorption are the major causes of capacitance dispersion at solid surfaces (Rahman *et al.* 1997). The analogous circuit, shown in Fig. 4, was utilized to study the impedance spectrum; it has shown a capacitive loop at high frequencies and the Warburg impedance at low frequencies (Khaled, 2010), (Ma *et al.* 2002). The emergence of the Warburg impedance in aerated acid solutions was thought to be owing to the diffusion of oxygen followed by its decrease (El Din *et al.* 2000). Due to the fact that the capacitive loops were depressed semi-circles rather than standard semi-circles, a constant phase element (CPE) was replaced for the capacitive element to provide a more precise match (Wu et al. 1999; Rahman *et al.*1997).

$$Z_{cpe} = \frac{1}{Y_0(j\omega)^n} \qquad (6)$$

where, Y_0 is the admittance of the corrosive system at 1 rads^{-1} and n is a constant (-1≤ n ≤1). When n = 0, the CPE represents a pure resistor, if n = -1, it represents an inductor and if n = +1, it represents a pure capacitor.

The corroding electrode's n values in both mediums are close to one, as shown in Table 2, confirming the CPE's almost capacitive behaviour. The idealized capacitance value (C_{id}) was determined using the equation (Mallaiya *et al.* 2011), (Van westing *et al.* 1993):

$$C_{id} = \frac{Y_0\omega^{n-1}}{\sin(\frac{n\pi}{2})} \qquad (7)$$

where, 'ω' is the angular frequency at the maximum value of the imaginary part of impedance -Z". The angular frequency and C_{dl} are calculated using the expressions (Hsu and Mansfeld, 2001):

$$\omega_{max} = \left(\frac{1}{R_{ct}Y_0}\right)^{1/n} \qquad (8)$$

$$C_{dl} = Y_0(\omega_{max})^{n-1} \qquad (9)$$

Due to an increase in the surface coverage by the inhibitor, there was an increase in R_{ct} with concentration. The decrease in C_{dl} was a result of the adsorption of the inhibitor molecule with water replacement at the metal/ solution interface, which led to a decrease in local dielectric constant and/or an increase in the thickness of the electrical double layer (Behpour *et al.* 2009). The gradual displacement of water molecules by the adsorption of the inhibitor onto the metal surface decreased the extent of the corrosion (Benabdellah *et al.* 2007).

3.3 Polarization Measurements

The addition of inhibitor to corrosive media has altered the anodic and cathodic Tafel slopes, as seen in Fig. 5 (a and b) polarisation curves, demonstrating its impact on the corresponding reactions. However, the impact was much stronger in the cathodic curve and the two curves were almost parallel, showing that the hydrogen evolution process was under activation control (Zarrouk *et al.* 2012). Because the greatest shift of E_{corr} in both the media in this investigation was less than 85 mV, the inhibitor may be classified as a mixed type (Zarrouk *et al.* 2012).

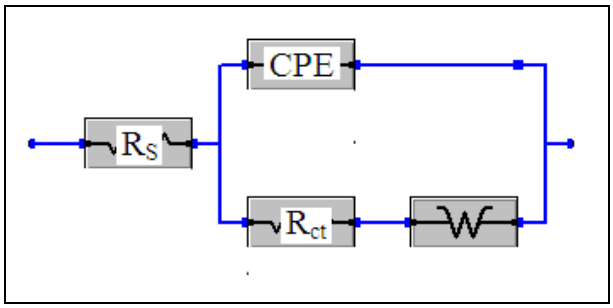

Fig. 4: Randles Equivalent Circuit

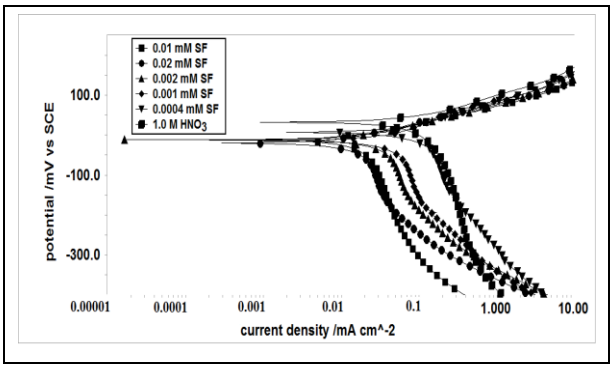

Fig. 5 a: Tafel plots for Cu in 1.0 M HNO_3 solution at various concentrations of sparfloxacin

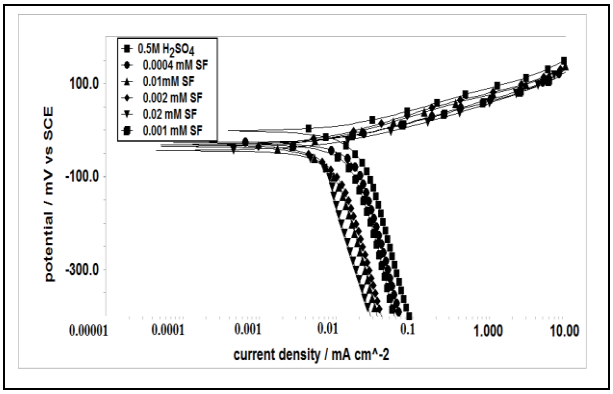

Fig. 5 b: Tafel plots for Cu in 0.5 M H_2SO_4 solution at various concentrations of sparfloxacin

Table 3. Electrochemical parameters for the corrosion of copper in 1 M HNO_3 and 0.5 M H_2SO_4 solutions at different concentrations of the inhibitor, derived from Tafel polarization curves

Medium	Concentration (mM)	E_{corr} (mV)	i_{corr} (μA cm^{-2})	β_c (mV)	β_a (mV)	Corrosion rate (mpy)	IE%
HNO_3	Blank	42.10	109	363.1	66.0	175.7	-
	0.0004	7.22	80.5	204.0	69.8	129.9	26
	0.001	-14.40	42.8	161.5	67.3	68.98	61
	0.002	-11.70	38.0	147.7	53.1	61.85	65
	0.01	-12.3	27.0	265.6	47.2	43.56	75
	0.02	-20.30	25.1	136.6	50.7	41.04	77
H_2SO_4	Blank	4.52	23.0	301.9	49.10	37.20	-
	0.0004	-26.80	17.0	374.6	49.30	28.13	26
	0.001	-29.80	11.3	382.9	47.70	18.37	51
	0.002	-43.20	6.60	601.3	44.50	10.68	71
	0.01	-35.20	5.18	242.2	49.60	8.37	77
	0.02	-31.50	4.15	212.9	48.80	7.84	82

In the anodic range, the Tafel polarisation curves have no sharp slope, indicating that no passive layer was produced on the copper surface. Copper is known to be transformed to Cu^{+2} and does not form an oxide coating in acid conditions, according to the Pourbaix diagram (Zarrouk *et al.* 2012). Cu does not dissolve into Cu^{+2} in de-aerated acid solutions, but it does so in the presence of dissolved oxygen, generating Cu^{+2} ion through the method described below:

Anodic reaction:

$$Cu \rightarrow Cu^{2+} + 2e^- \quad (10)$$

Cathodic reaction:

$$O_2 + 4H^+ + 4e^- \rightarrow 2H_2O \quad (11)$$

The migration of soluble Cu^{+2} species from the outer Helmholtz plane to the bulk solution controls the dissolution of copper (Zarrouk *et al.* 2012).

The electrochemical parameters such as corrosion potential (E_{corr}), corrosion current (i_{corr}), cathodic and anodic Tafel slopes and inhibitor efficiencies are listed in Table 3. The higher β_c in comparison with β_a in Table 3 has shown a higher influence on the retardation of cathode reduction rate than anodic metal dissolution, though β_c and β_a change with an increase in inhibitor concentration (Sanghvi *et al.* 1999). This means that sparfloxacin has slowed down the cathodic process more than the anodic dissolution. In a sulphuric acid solution, it has inhibited copper dissolution more effectively than in a nitric acid solution.

3.4 Adsorption Isotherm

Sparfloxacin molecule adsorption at the metal solution interface may be thought of as a replacement process in which an organic substance (Org_{sol}) from the aqueous medium replaces the water molecules connected with the metal surface (H_2O_{ads}).

$$Org_{(sol)} + xH_2O_{ads} \rightarrow Org_{ads} + xH_2O \quad (12)$$

where, 'x' is the number of water molecules replaced by the adsorption of one sparfloxacin molecule. Using the R_{ct} values, the surface coverage (θ) of the inhibitor was calculated using the relation,

$$\theta = \frac{R'_{ct} - R_{ct}}{R'_{ct}} \quad (13)$$

where, R'_{ct} and R_c are the charge transfer resistance values in the inhibited and blank solutions, respectively. Analysis showed that the adsorption followed Langmuir isotherm, given by the expression (Mallaiya *et al.* 2011), (Zarrouk *et al.* 2012), (Joseph and Joseph, 2011):

$$C_{inh}/\theta = C_{inh} + 1/K_{ads} \quad (14)$$

where, C_{inh} is the concentration of the inhibitor, θ is the surface coverage and K_{ads} is the adsorption equilibrium constant. At constant temperature, the value of K_{ads} is determined from the plot of C_{inh} vs. C_{inh}/θ.

The standard free energy of adsorption was calculated using the expression:

$$K_{ads} = 1/55.5 \exp^{-\Delta G/RT} \quad (15)$$

where, T is the thermodynamic temperature, R is the universal gas constant, ΔG is the free energy of adsorption and 55.5 is the concentration of water in the solution in mol L^{-1}.

Langmuir adsorption isotherm for the adsorption of sparfloxacin on the copper metal surface in 1.0 M HNO_3 and 0.5 M H_2SO_4 solutions are shown in Fig. 6. The plots obtained were linear with correlation coefficients greater than 0.9. The calculated values of ΔG_{ads} at room temperature in nitric acid and sulphuric acid solutions are -45.96 kJmol^{-1} and -45.46 kJmol^{-1}, respectively. The negative values of ΔG_{ads} indicate the

spontaneous adsorption of sparfloxacin molecules onto the metal surface. In the present study, the values of ΔG_{ads} were greater than 40 $kJmol^{-1}$, indicating that the sparfloxacin molecules were getting adsorbed onto the metal surface by chemisorption (Bentiss *et al.* 1999).

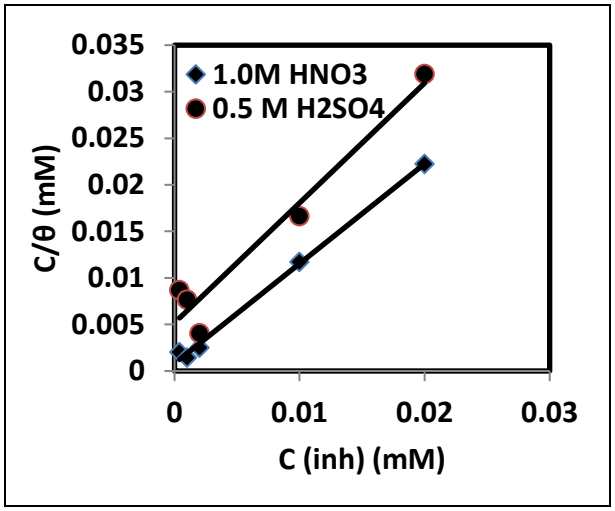

Fig. 6: Langmuir adsorption isotherm for the adsorption of sparfloxacin on the copper metal surface in 1.0 M HNO_3 and 0.5 M H_2SO_4 solutions

3.5 Effect of Temperature

Table 4 lists the various electrochemical parameters determined at various temperatures. It can be inferred from the table that with the rise in temperature, the inhibitor efficiency and corrosion rate has increased. Increased inhibitor efficiency means that the surface area covered by the inhibitor molecule has grown, slowing the rate of disintegration.

Fig. 7 and Fig. 8 exhibit Arrhenius plots and Transition state plots, respectively. The values of E_a measured in the presence of sparfloxacin were lower than those measured in the blank solution (Table 5), indicating that the energy barrier for inhibitor molecule adsorption on a copper surface has decreased. The surface area covered by the inhibitor molecule was growing with the rise in temperature, and the rate of metal dissolution in corrosive fluids was regulated by corrosion product diffusion through the inhibitor molecule's protective coating (Szauer and Brandt, 1981). The fact that E_a decreased when inhibitor molecules were added to both fluids has indicated that the inhibitor molecules were chemisorption-adsorbed onto the metal surface. (Szauer and Brandt, 1981), (Ivanov, 1986), (Ma *et al.* 2003), (Solmaz *et al.* 2008). The active state has more association and less disorder, as shown by the negative entropy value. The fact that ΔH is negative indicates that adsorption is an exothermic process.

Table 3. Electrochemical parameters from Tafel polarization curves for the corrosion of copper in 1.0 M HNO_3 and 0.5 M H_2SO_4 solutions at different temperatures

Medium	Concentration (mM)	Temperature (K)	E_{corr} (mV)	i_{corr} $\mu A/cm^2$	β_c (mV)	β_a (mV)	Corrosion rate (mpy)	IE %
HNO_3	Blank	308	2.59	30.3	173.6	54.40	49.04	-
	Blank	318	10.80	199.0	411.4	65.70	322.6	-
	Blank	328	21.70	358.0	440.0	59.90	579.2	-
	0.02 mM	308	6.420	14.8	373.6	77.7	23.90	51
	0.02 mM	318	8.890	72.8	330.3	61.0	117.8	63
	0.02 mM	328	14.10	94.8	415.3	63.0	153.5	74
H_2SO_4	Blank	308	-14.00	12.2	537.3	49.10	19.82	-
	Blank	318	-46.67	30.4	281.0	50.23	49.19	-
	Blank	328	11.70	88.5	271.9	62.89	143.2	-
	0.02 mM	308	-54.9	7.030	104.8	45.30	14.65	42
	0.02 mM	318	-31.8	12.60	219.2	46.0	20.45	59
	0.02 mM	328	-39.9	16.44	193.2	46.4	26.59	81

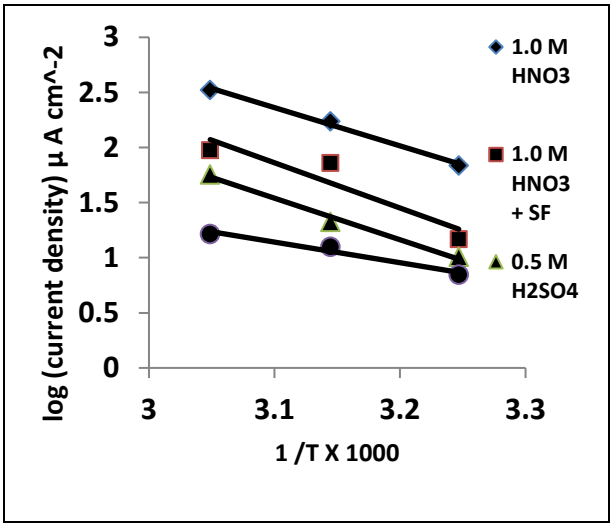

Fig. 7: Typical Arrhenius plots for corrosion of Cu in 1.0 M HNO_3 and 0.5 M H_2SO_4 solution

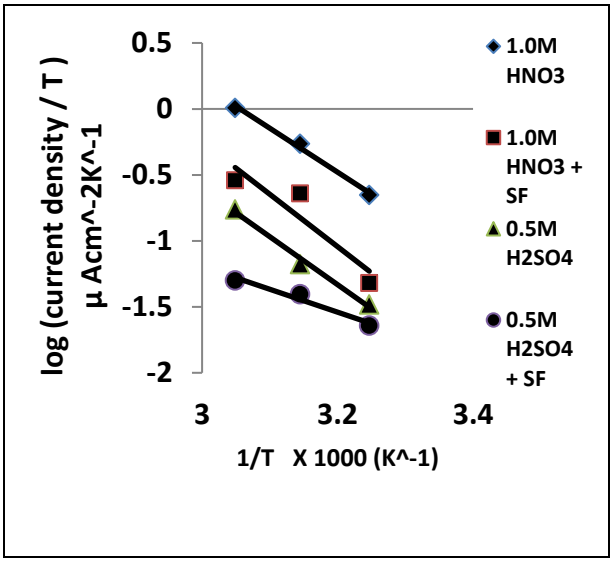

Fig. 8: Transition state plots for corrosion of Cu in 1.0 M HNO_3 and 0.5 M H_2SO_4 solution

Table 4. Thermodynamic parameters obtained from potentio-dynamic polarization studies

Medium	Inhibitor concentration (mM)	K_{ads} (M^{-1})	ΔG_{ads} kJ/mole	ΔH kJ/mole	ΔS (J/mole/K)	E_a (kJ/mole)	R
HNO_3	Blank	-	-	-63.7	-26.8	66.44	0.993
	0.02	1807174	-45.96	-56.7	-70.2	59.39	0.866
H_2SO_4	Blank	-	-	-69.5	-38.2	72.19	0.989
	0.02	1478764	-45.46	-33.1	-120.7	35.80	0.858

The fact that H was negative has indicated that the adsorption was an exothermic process. The active state has more association and less disorder, as shown by the negative entropy change value. The inhibitor molecule may freely move in the bulk solution prior to adsorption, but as adsorption progressed, inhibitor molecules were adsorbed in an organized way onto the metal surface, lowering entropy (Szauer & Brand, 1981).

3.6 Potential of Zero Charge (PZC)

The open circuit potential with respect to the PZC determines the metal's surface charge (Ramesh Saliyan and Adhikari, 2008). Fig. 9 a and Fig. 9 b have demonstrated the dependence of the double-layer capacitance on the applied DC potential in nitric acid and sulphuric acid in the absence and presence of sparfloxacin. Table 6 contains the E_{ocp} and PZC data.

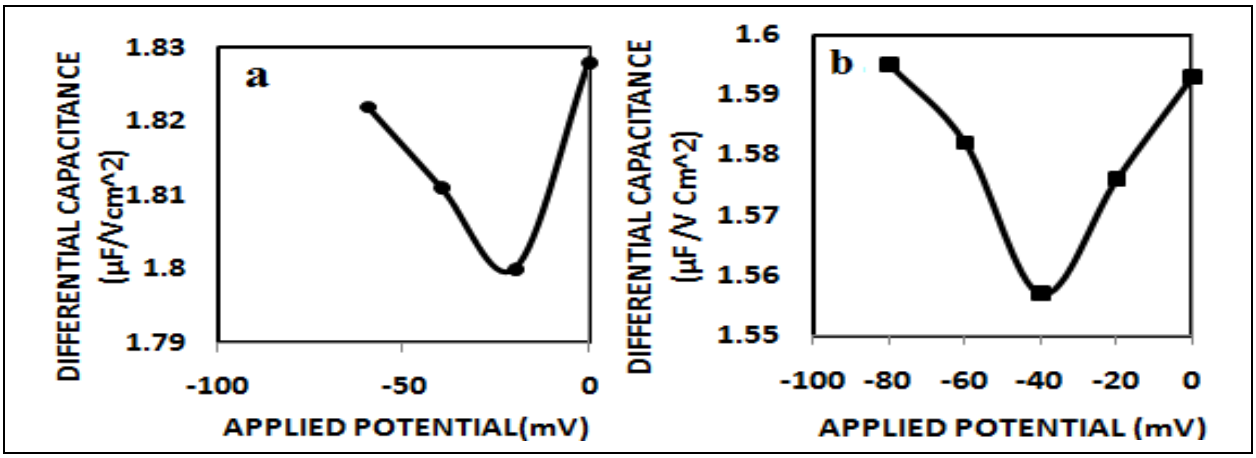

Fig. 9: Plot of differential capacitance vs. applied potential for copper in: (a) 0.5 M H_2SO_4 and (b) 0.5 M H_2SO_4, containing 0.01 mM sparfloxacin

Table 5. Excess charge on Cu electrode in 1.0 M HNO_3 and 0.5 M H_2SO_4 solutions in the presence and absence of the inhibitor

Medium	E_{OCP} (mV/SCE)	E_{PZC} (mV/SCE)	Excess charge, E_{OCP} -E_{PZC} (mV)
1.0 M HNO_3	+42.10	+40	+2.1
1.0 M HNO_3 + 0.01 mM of inhibitor	-12.3	-20	+7.7
0.5 M H_2SO_4	+4.52	-20	+24.52
0.5 M H_2SO_4 + 0.01 mM of inhibitor	-35.2	-40	+4.8

As seen from Table 6, the metal surface was positively charged with respect to PZC, based on which the mechanism proposed was that the sulphate and nitrate ions will first get adsorbed onto the metal surface (Ramesh Saliyan and Adhikari, 2008), (Popova, 2003), (Solmaz *et al.* 2008) and the protonated inhibitor molecules make the bond with the anions, preventing the metal dissolution (Doner *et al.* 2011).

3.7 Synergistic Effect of Halide Ions

Due to synergy, the inhibitor efficacy of a mixture of two or more corrosion inhibitors applied to a corrosive environment of metal may be larger than the total of each of the additions.

The surface charge of copper at the OCP was shown to be positive in the presence of halide ions in sulphuric acid and nitric acid solutions, and the mechanism hypothesized was that the halide ions (X^-) would first become adsorbed onto the metal surface (Ramesh Saliyan and Adhikari, 2008), (Popova, 2003), (Solmaz *et al.* 2008) and the protonated inhibitor molecules (HI^+) will form a bond with the anions and prevent metal dissolution (Doner *et al.* 2011), as shown in Equations 16 and 17.

Table 7. Electrochemical parameters for copper in 1 M HNO_3 and 0.5 M H_2SO_4 solutions in the presence of KCl, KBr and KI

Medium	Inhibitor Concentration (mM)	Y_0 (x 10^{-6}) $\Omega^{-1}cm^{-2}$	n	R_{ct} Ωcm^2	θ	S_θ
1.0 M HNO_3	Blank	862.9	0.997	87	-	-
	0.002 mM SF	192.7	0.922	191	0.5445	-
	0.5 mM KCl	189.1	0.898	313	0.7220	-
	0.002 mM SF+ 0.5 mM KCl	53.50	0.973	495.9	0.8245	0.7213
	0.5 mM KBr	271.0	0.912	231.8	0.6246	-
	0.002 mM SF+ 0.5 mM KBr	140.2	0.967	456	0.8092	0.8957
	0.5 mM KI	99.5	0.905	123	0.2926	-
	0.002 mM SF+ 0.5 mM KI	110.2	0.925	948.7	0.9082	3.50
0.5 M H_2SO_4	Blank	330	0.930	63	-	-
	0.002 mM SF	203.7	0.921	387	0.7751	-
	0.5 mM KCl	349.1	0.945	191	0.6701	-
	0.002 mM SF+ 0.5 mM KCl	359.2	0.945	248.6	0.7465	0.2923
	0.5 mM KBr	256.7	0.934	154	0.5909	-
	0.002 mM SF+ 0.5 mM KBr	153.2	0.963	606	0.8960	0.8846
	0.5 mM KI	152.6	0.926	174	0.6379	-
	0.002 mM SF+ 0.5 mM KI	70.3	0.939	2228	0.9717	2.87

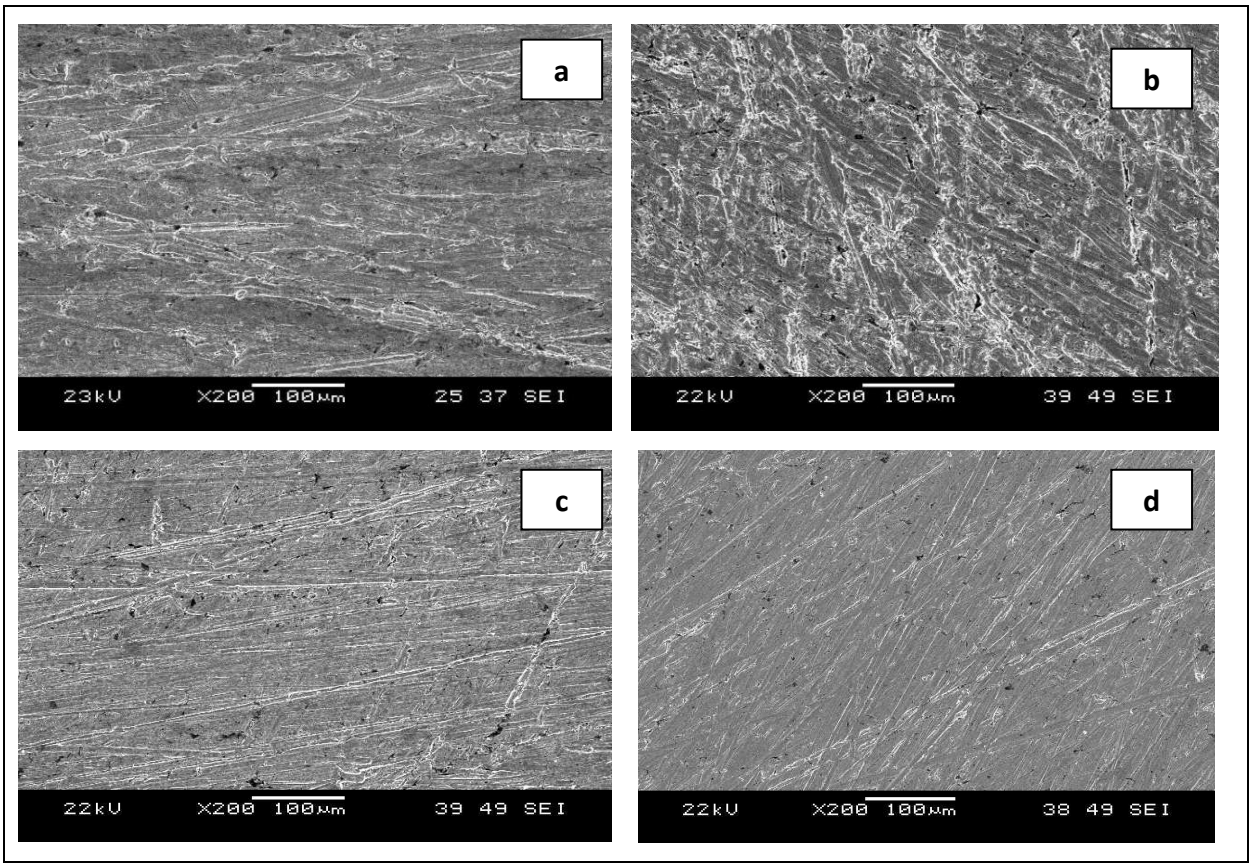

Fig. 10: SEM micrographs of copper specimens after immersion in: (a) 1.0 M HNO_3 (b) 0.5 M H_2SO_4 (c) 1.0 M HNO_3 containing sparfloxacin and d) 0.5 M H_2SO_4 containing sparfloxacin

$$X^-_S \quad \_ \quad X^-_{ads} \qquad (16)$$

$$X^-_{ads} + HI^+_S \quad \_ \quad (X^- - HI^+)_{ads} \qquad (17)$$

Thus, the halide ions were able to improve adsorption of the organic cations by forming intermediate bridges between the positively charged metal surface and the positive end of the organic inhibitor and result in increased surface coverage (Özcan *et al.* 2008), (Zhao and Chen, 2012), (Feng *et al.* 1999), (Obot *et al.* 2009), (Umoren *et al.* 2010), (Umoren *et al.* 2008), (Pavithra, *et al.* 2010), (Ai *et al.* 2006). The synergism parameters S_θ calculated using the impedance studies with the addition of potassium chloride, potassium bromide and potassium iodide are shown in Table 7. In the present case, the addition of iodide ions has given S_θ values of 3.50 and 2.87 in nitric acid and sulphuric acid media, respectively and has shown a synergistic effect in both the acid media. The greater influence of the iodide ion was often attributed to its large ionic radius, high hydrophobicity and low electronegativity (Bentiss *et al.* 2002), which has helped in the adsorption of the inhibitor molecules onto the metal surface (Ramesh Saliyan and Adhikari, 2008).

3.8 Surface Morphology

Figures 10 a and 10 b have shown SEM micrographs of copper specimens subjected to acid solutions. These images have clearly shown the high-density pits caused by copper exposure in acid environments. Figures 10 c and 10 d have depicted the effects of adding 0.01 mM sparfloxacin to the corrosive medium, revealing the creation of a protective coating on the copper specimen's surface when sparfloxacin was present. The absence of pitting in the micrographs can be ascribed to the inhibitor molecules' adsorption on the metal surface, which provided the protection.

4. CONCLUSION

(i) The inhibitor efficiency has improved with increasing sparfloxacin concentration in both nitric acid and sulphuric acid media, with nearly 90% efficiency found at 0.02 mM dosage. The results have suggested that sparfloxacin can operate as an excellent copper corrosion inhibitor in both acid and alkaline environments.

(ii) The chemical was functioning as a mixed kind of inhibitor, according to the potentio-dynamic polarisation curves.

(iii) Sparfloxacin adsorption on metal surfaces has followed the Langmuir adsorption isotherm.

(iv) If the free energy of adsorption was more than -40 $kJmol^{-1}$, chemisorption was the mode of adsorption; this was further supported by the fact that the presence of inhibitors has reduced E_a.

(v) The production of sulphate and nitrate interconnecting bridges in the adsorption of the inhibitor onto the metal surface in both acid and alkaline conditions was confirmed by PZC determination.

(vi) The negative sign of ΔH_{ads} has indicated that the adsorption of inhibitor molecule was an exothermic process. The negative value of ΔS_{ads} in the presence of the inhibitor has revealed that the active state has more association and less disorder.

ACKNOWLEDGEMENT

The authors gratefully acknowledge the facilities provided by the Principal and the Management of Coimbatore Institute of Technology, India and PSG College of Technology, Coimbatore, India.

FUNDING

This research received no specific grant from any funding agency in the public, commercial, or not-for-profit sectors.

CONFLICTS OF INTEREST

The authors declare that there is no conflict of interest.

COPYRIGHT

REFRENCES

Ai, J., Guo, X., Qu, J., Chen, Z. and Zheng, J., Adsorption behavior and synergistic mechanism of a cationic inhibitor and KI on the galvanic electrode, *Colloids and Surfaces A: Physicochemical and Engineering Aspects*, 281(1), 147-155(2006). https://doi.org/10.1016/j.colsurfa.2006.02.031

Aramaki, K. and Hackerman, N., Inhibition mechanism of medium-sized polyethyleneimine, *J. Electrochem. Soc.*, 116(5), 568-574(1969). https://doi.org/10.1149/1.2411965

Behpour, M., Ghoreishi, S., Gandomi-Niasar, A., Soltani, N. and Salavati-Niasari, M., The inhibition of mild steel corrosion in hydrochloric acid media by two Schiff base compounds, *J. Mater. Sci*., 44(10), 2444-2453(2009). https://doi.org/10.1007/s10853-009-3309-y

Benabdellah, M., Touzani, R., Aouniti, A., Dafali, A., El Kadiri, S., Hammouti, B. and Benkaddour, M., Inhibitive action of some bipyrazolic compounds on the corrosion of steel in 1M HCl: Part I: Electrochemical study, *Mater. Chem. Phys*., 105(2), 373-379(2007). https://doi.org/10.1016/j.matchemphys.2007.05.001

Bentiss, F., Bouanis, M., Mernari, B., Traisnel, M. and Lagrenee, M., Effect of iodide ions on corrosion inhibition of mild steel by 3, 5-bis (4-methylthiophenyl)-4H-1, 2, 4-triazole in sulfuric acid solution', *J. Appl. Electrochem*., 32(6), 671-678(2002). https://doi.org/10.1023/A:1020161332235

Bentiss, F., Traisnel, M., Gengembre, L. and Lagrenée, M., A new triazole derivative as inhibitor of the acid corrosion of mild steel: electrochemical studies, weight loss determination, SEM and XPS', *Applied surface science*, 152(3), 237-249(1999). https://doi.org/10.1016/S0169-4332(99)00322-0

Döner, A., Solmaz, R., Özcan, M. and Kardaş, G., Experimental and theoretical studies of thiazoles as corrosion inhibitors for mild steel in sulphuric acid solution', *Corros. Sci*., 53(9), 2902-2913(2011). https://doi.org/10.1016/j.corsci.2011.05.027

El-Din, A. S., El Dahshan, M. and El-Din, A. T., Dissolution of copper and copper-nickel alloys in aerated dilute HCl solutions, *Desalination*, 130(1), 89-97(2000). https://doi.org/10.1016/s0011-9164(00)00077-1

Feng, Y., Siow, K., Teo, W. and Hsieh, A., The synergistic effects of propargyl alcohol and potassium iodide on the inhibition of mild steel in 0.5 M sulfuric acid solution, *Corros. Sci*., 41(5), 829-852(1999). https://doi.org/10.1016/S0010-938X(98)00144-9

Hsu, C. and Mansfeld, F., Technical note: concerning the conversion of the constant phase element parameter Y_0 into a capacitance, *Corros. Sci*., 57(9), 747-748(2001). https://doi.org/10.5006/1.3280607

Ivanov, E., Inhibitors for metal corrosion in acid media, Metallurgy, Moscow(1986).

Joseph, B. and Joseph, A., Inhibition of Copper Corrosion in 1 M Nitric Acid-Electro Analytical and Theoretical Study with (E)-(4-(4-Methoxybenzylideneamino)-4H-1, 2, 4-Triazole-3, 5diyl) Dimethanol (MBATD), *Portugaliae Electrochimica*. *Acta*., 29(4), 253-271(2011). https://doi.org/10.4152/pea.201104253

Khaled, K., Corrosion control of copper in nitric acid solutions using some amino acids–A combined experimental and theoretical study, *Corros. Sci*., 52(10), 3225-3234(2010). https://doi.org/10.1016/j.corsci.2010.05.039

Ma, H., Chen, S., Niu, L., Zhao, S., Li, S. and Li, D., Inhibition of copper corrosion by several Schiff bases in aerated halide solutions, *J. Appl. Electrochemi*cal., 32(1), 65-72(2002). https://doi.org/10.1023/A:1014242112512

Ma, H., Chen, S., Yin, B., Zhao, S. and Liu, X., Impedance spectroscopic study of corrosion inhibition of copper by surfactants in the acidic solutions, *Corros. Sci*., 45(5), 867-882(2003). https://doi.org/10.1016/S0010-938X(02)00175-0

Mallaiya, K., Subramaniam, R., Srikandan, S. S., Gowri, S., Rajasekaran, N and Selvaraj, A., Electrochemical characterization of the protective film formed by the unsymmetrical Schiff's base on the mild steel surface in acid media, *Elect. Acta*, 56(11), 3857-3863(2011). https://doi.org/10.1016/j.electacta.2011.02.036

Obot, I., Obi-Egbedi, N. and Umoren, S., The synergistic inhibitive effect and some quantum chemical parameters of 2,3-diaminonaphthalene and iodide ions on the hydrochloric acid corrosion of aluminium, *Corros. Sci*., 51(2), 276-282(2009). https://doi.org/10.1016/j.corsci.2008.11.013

Özcan, M., Solmaz, R., Kardaş, G. and Dehri, I., Adsorption properties of barbiturates as green corrosion inhibitors on mild steel in phosphoric acid, *Colloids and Surfaces A: Physicochemical and Engineering Aspects*, 25(1-2), 57-63(2008). https://doi.org/10.1016/j.colsurfa.2008.04.031

Pavithra, M., Venkatesha, T., Vathsala, K. and Nayana, K., Synergistic effect of halide ions on improving corrosion inhibition behaviour of benzisothiozole-3-piperazine hydrochloride on mild steel in 0.5 M H_2SO_4 medium, *Corros. Sci*., 52(11), 3811-3819(2010). https://doi.org/10.1016/j.corsci.2010.07.034

Popova, A., Sokolova, E., Raicheva, S. and Christov, M., AC and DC study of the temperature effect on mild steel corrosion in acid media in the presence of benzimidazole derivatives, *Corros. Sci*., 45(1), 33-58(2003).

Rahman, K. M., Schneider, S. C. and Seitz, M. A., Hopping and Ionic Conduction in Tin Oxide-Based Thick-Film Resistor Compositions, *J. Am. Ceram. Soc*., 80(5), 1198-1202(1997). https://doi.org/10.1111/j.1151-2916.1997.tb02964.x

Şahin, M., Bilgic, S. and Yılmaz, H., The inhibition effects of some cyclic nitrogen compounds on the corrosion of the steel in NaCl mediums, *Appl. Surf. Sci.*, 195(1), 1-7(2002). https://doi.org/10.1016/S0169-4332(01)00783-8

Saiyan, V. R. and Adhikari, A. V., Quinolin-5-ylmethylene-3-{[8-(trifluoromethyl) quinolin-4-yl] thio} propanohydrazide as an effective inhibitor of mild steel corrosion in HCl solution, *Corros. Sci*., 50(1), 55-61(2008). https://doi.org/10.1016/j.corsci.2006.06.035

Sanghvi, M., Shukla, S., Misra, A., Padh, M. and Mehta, G., Inhibition of hydrochloric acid corrosion of mild steel by aid extracts of Emblica officianalis, Terminalia bellirica and Terminalia chebula, *Bulletin of Electrochemistry*, 13(8-9), 358-361(1997).

Solmaz, R., Kardaş, G., Culha, M., Yazıcı, B. and Erbil, M., Investigation of adsorption and inhibitive effect of 2-mercaptothiazoline on corrosion of mild steel in hydrochloric acid media, *Electrochimica Acta*, 53(20), 5941-5952(2008). https://doi.org/10.1016/j.electacta.2008.03.055

Szauer, T. and Brandt, A., Adsorption of oleates of various amines on iron in acidic solution, *Electrochimica Acta*, 26(9), 1253-1256(1981). https://doi.org/10.1016/0013-4686(81)85107-9

Umoren, S., Li, Y. and Wang, F., Synergistic effect of iodide ion and polyacrylic acid on corrosion inhibition of iron in H_2SO_4 investigated by electrochemical techniques, *Corros. Sci.*, 52(7), 2422-2429(2010). https://doi.org/10.1016/j.corsci.2010.03.021

Umoren, S., Ogbobe, O., Igwe, I. and Ebenso, E., Inhibition of mild steel corrosion in acidic medium using synthetic and naturally occurring polymers and synergistic halide additives, *Corros. Sci*., 50(7), 1998-2006(2008). https://doi.org/10.1016/j.corsci.2008.04.015

Van Westing, E., Ferrari, G. and De Wit, J., The determination of coating performance with impedance measurements-I. Coating polymer properties, *Corros. Sci*., 34(9), 1511-1530(1993). https://doi.org/10.1016/0010-938x(93)90245-c

Wu, X., Ma, H., Chen, S., Xu, Z. and Sui, A., General equivalent circuits for faradaic electrode processes under electrochemical reaction control, *J. Electrochem. Soc.*, 146(5), 1847-1853(1999). https://doi.org/10.1149/1.1391854

Zarrouk, Hammouti, B., Zarrok, H., Bouachrine, M., Khaled, K. and Al-Deyab, S., Corrosion inhibition of copper in nitric acid solutions using a new triazole derivative, *Int. J. Electrochem. Sci.*, 7(1), 89-105(2012).

Zhao, J. and Chen, G., The synergistic inhibition effect of oleic-based imidazoline and sodium benzoate on mild steel corrosion in a CO_2-saturated brine solution, *Electrochimica Acta*, 69, 247-255(2012). https://doi.org/10.1016/j.electacta.2012.02.101